Brazilian Dental Journal. Volume 37 (2026), e26-7049
http://dx.doi.org/10.1590/0103-644020267049

ISSN 0103-6440

Dental implants near internally resorpted roots: comparison between CBCT exam and periapical radiography

Débora Costa Ruiz [1,2], Maria Fernanda Silva Andrade-Bortoletto [1], Sergio Lins de-Azevedo-Vaz [2], Deborah Queiroz Freitas [1].

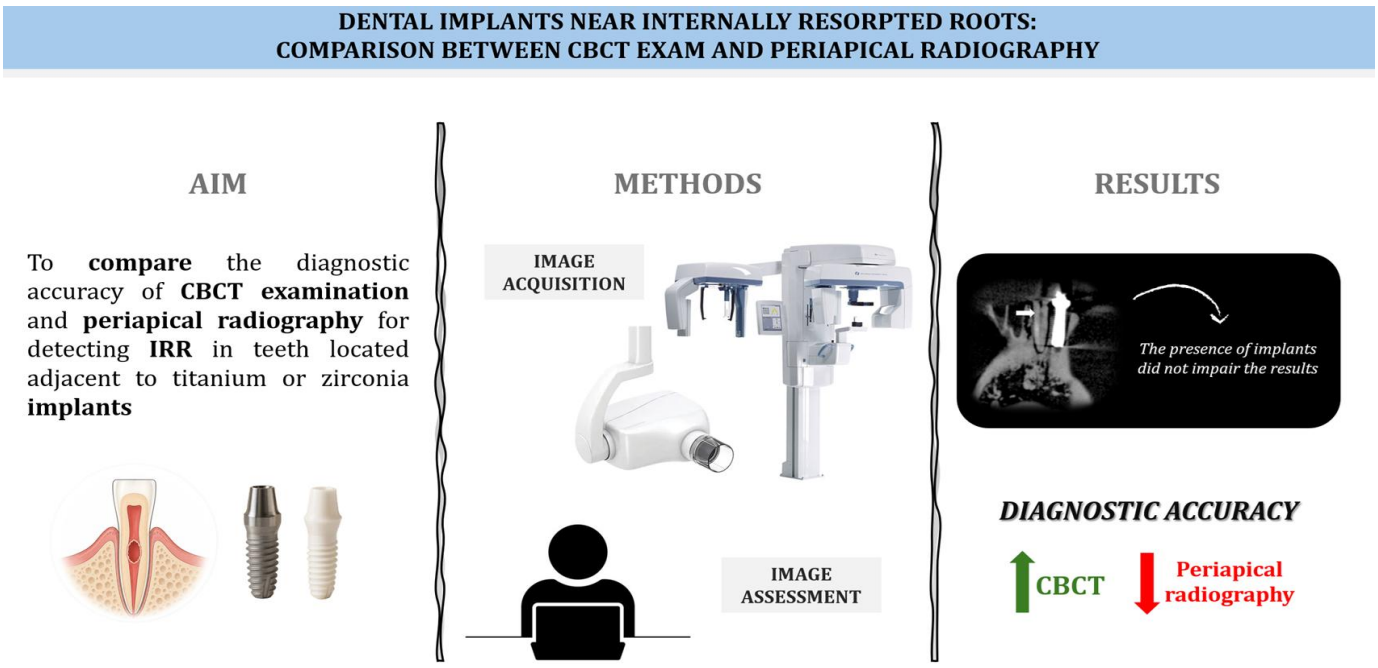
[1]Department of Oral Diagnosis, Piracicaba Dental School, University of Campinas, Piracicaba, SP, Brazil

[2]Department of Dental Clinic, Federal University of Espírito Santo, Vitória, ES, Brazil.

Correspondence: Débora Costa Ruiz – Department of Oral Diagnosis, Piracicaba Dental School, University of Campinas, Av. Limeira, 901, Areião, Zip-Code 13414-903, Piracicaba, SP, Brazil 55-19-21065227
E-mail: ruiz03338@gmail.com

This study compared the diagnostic accuracy of cone-beam computed tomography (CBCT) and periapical radiography for detecting internal root resorption (IRR) in teeth adjacent to titanium or zirconia implants. Twenty single-rooted teeth (10 with IRR and 10 without) were individually placed in a human mandible. Periapical radiographs and CBCT exams were obtained with and without a titanium or zirconia implant. Radiographs were acquired with a photostimulable phosphor plate receptor at 70 kVp, 7 mA, and 0.160 s. CBCT scans were acquired at 90 kVp, 8 mA, 0.085mm3 voxel size, and 5×5cm field of view. Four examiners independently evaluated the radiographs and the CBCT exams. The area under the receiver operating characteristic curve (AUC), sensitivity, and specificity values were calculated and compared using two-way ANOVA (α = 5%). Inter- and intraexaminer agreement for IRR diagnosis was assessed using weighted Kappa. CBCT demonstrated significantly higher AUC (p=0.007), sensitivity (p=0.009), and specificity (p=0.037) for IRR detection compared with periapical radiographs, regardless of implant presence or type. The presence of an implant did not influence the results. Intraexaminer agreement ranged from moderate to almost perfect (0.48–0.95), and interexaminer agreement ranged from fair to almost perfect (0.30–0.85). CBCT demonstrated higher diagnostic accuracy than periapical radiography for detecting IRR, even in the presence of adjacent titanium or zirconia implants, as implant-related artifacts did not impair image interpretation. Therefore, when periapical radiography is insufficient to establish a diagnosis, the use of CBCT may be clinically justified despite the additional radiation exposure.

Key Words: Cone-beam computed tomography, dental radiography, artifact, dental implant, root resorption.



Introduction

Internal root resorption (IRR) is a progressive and destructive lesion characterized by the loss of dentin within the root canal space (1). Although often asymptomatic in its early stages, IRR can compromise the tooth's structural integrity if not diagnosed and treated promptly, ultimately jeopardizing prognosis (2). The condition is triggered by odontoclastic activity resulting from trauma, bacterial infection, orthodontic movement, intracoronal bleaching, among others (3). Since IRR is typically silent until it becomes extensive, early detection plays a crucial role in ensuring favorable treatment outcomes (2).

The diagnosis of IRR is supported by imaging examinations such as periapical radiographs and cone beam computed tomography (CBCT) (4). While widely accessible, radiographs are inherently limited by their two-dimensional nature, which often results in superimposition of anatomical structures. This overlap may conceal early-stage IRR, making it difficult to identify, and for that reason, the American Association of Endodontics recommends the use of CBCT for endodontic purposes (5). In that matter, CBCT has emerged as an important adjunct method in endodontic imaging, allowing multiplanar visualization without superimposition and improving the detection of resorptive defects (1). Multiple studies have shown CBCT's superior sensitivity for identifying root resorption and assessing its true size and extent compared with radiographs (6-8).

However, CBCT image quality can be adversely affected by high-density materials because they induce beam-hardening artifacts (9). Metallic posts in adjacent teeth can impair the detection of IRR on CBCT images (10). Similarly, dental implants are artifact-inducing materials that may compromise visualization and, consequently, the diagnosis of neighboring dental structures (11,12). Previous studies have shown that nearby implants or restorations can impair or fail to improve the diagnosis of root fractures, caries lesions, and peri-implant defects on CBCT, indicating that this modality does not always outperform conventional imaging exams (13-15). However, its specific impact on detecting IRR has not yet been established. Because IRR presents distinct imaging characteristics, typically appearing as a smooth enlargement of the root canal with an oval or round shape, findings from these other diagnostic tasks cannot be directly extrapolated to IRR (6).

Considering that CBCT delivers substantially higher X-ray doses than periapical radiographs, its use should be carefully justified under the ALADAIP principle (“As Low As Diagnostically Acceptable, being Indication-oriented and Patient-specific”) (16). Therefore, understanding whether implant-induced artifacts significantly compromise IRR detection on CBCT is essential for guiding appropriate imaging selection and preventing unnecessary radiation to the patient. In this context, it is important to understand whether periapical radiographs, despite their inherent limitations, might offer a more reliable diagnostic than CBCT when suspecting IRR in teeth adjacent to implants. Therefore, this study aimed to compare the diagnostic accuracy of periapical radiographs and CBCT for detecting IRR in teeth adjacent to titanium and zirconia implants.

Materials and Methods

This research was conducted after approval of the local institutional review board under the protocol number CAAE 83781224.5.0000.5418 and complied with the Helsinki Declaration.

Sample selection and preparation

A dry human mandible with intact alveolar sockets and 20 single-rooted human teeth were used in this study. The teeth were obtained from non-vulnerable patients who underwent extraction for clinical reasons unrelated to the research. After extraction, the teeth were cleaned to remove soft tissue remnants and stored in a 2% glutaraldehyde solution to prevent microbial growth. Only permanent teeth with fully formed roots were included. Teeth were excluded if they showed evidence of previous endodontic treatment, internal or external root resorption, root fractures, extensive caries lesions, canal obliteration, or pulp calcifications. All teeth were evaluated by visual and radiographic inspection to confirm eligibility according to the inclusion and exclusion criteria.

Initially, each crown was separated from its respective root at the cementoenamel junction using an Isomet diamond disc (Isomet 1000, Buehler Ltd., Lake Bluff, USA). Afterward, all roots were longitudinally sectioned in the mesiodistal direction, yielding two segments (buccal and lingual). This procedure prevented potential bias during evaluation, ensuring that examiners would not assume that only sectioned teeth contained IRR defects.

Ten roots were designated for the control group, while the other ten were assigned to the IRR group, in which root resorptions were simulated based on mechanical and biochemical procedures described in previous studies (17,18). Cavities measuring 0.25 mm in diameter and 0.25 mm in depth were created in the internal surface of the buccal root canal wall using a 0.25-mm spherical carbide bur (KG Sorensen, Cotia, Brazil), selected to standardize the cavity diameter. Cavity depth was controlled using a periodontal probe with millimeter markings. The cavities were prepared carefully to preserve the remaining root canal walls and simulate an early-stage IRR. Moreover, the other root canal surfaces were not instrumented, as larger lesions would be more readily detectable.

Following cavity preparation, a cylindrical chamber made of composite resin (Z250; 3M ESPE, St. Paul, MN, USA) was positioned and adapted over the prepared cavity on the internal surface of the buccal root canal wall to delimit the demineralization area and confine the application of a chemical agent. For that, the chamber was placed in direct contact with the root surface surrounding the standardized cavity, restricting 5% nitric acid to the intended area, thereby minimizing leakage to adjacent surfaces. The acid was maintained in contact with the cavity for 48 h at 1°C (±3°C) throughout the induction period. After demineralization, the composite resin chamber was removed, residual materials were rinsed away under running water, and the two dental halves were reattached using cyanoacrylate adhesive (Figure 1) (Scotch Super Glue, 3M, Maplewood, MN, USA).

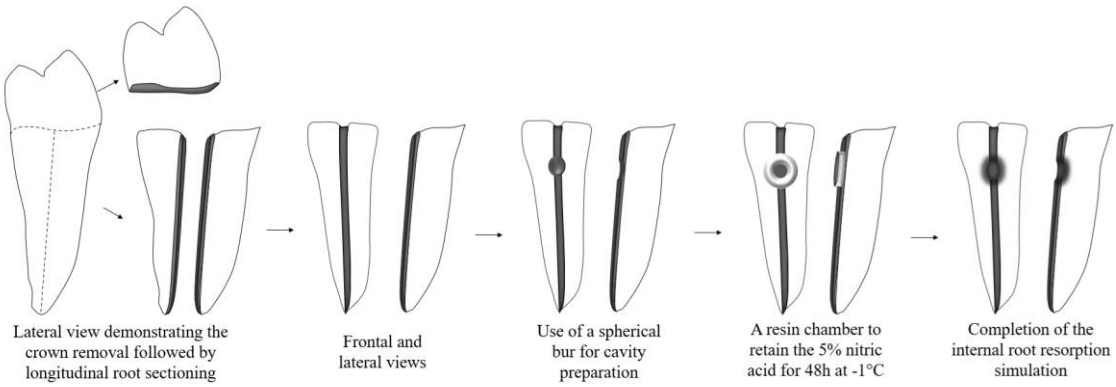


Figure 1. Illustrative description of the steps followed to simulate internal root resorption

Image acquisition

A Rinn XCP receptor holder (Dentsply Sirona, Pennsylvania, USA) was used to ensure standardized radiographic geometry for the acquisition of periapical radiographs, consisting of a 30 cm focus-to-receptor distance and a 1.5 cm mandible-to-receptor distance. Moreover, the mandible was covered with utility wax (15 mm thick) to simulate the attenuation of the X-ray beam by the patient's soft tissues.

Radiographs of each tooth positioned individually in the empty socket of the left mandibular lateral incisor were acquired using a Focus intraoral X-ray unit (Instrumentarium Dental, Tuusula, Finland) and a new photostimulable phosphor (PSP) plate receptor from the Express system (Instrumentarium Dental, Tuusula, Finland). Exposure parameters were set at 70 kVp, 7 mA, and 0.160 s, resulting in radiographs with standardized brightness and contrast.

The radiographs were obtained in three conditions: (1) without any adjacent implant; (2) with a titanium implant (Titamax, Neodent, Brazil) placed adjacent to the root, in the left mandibular canine region; and (3) with a zirconia implant (Z-Look3, Z-Systems, Switzerland)

positioned in the same location. Sixty periapical radiographs were obtained (20 roots × 3 conditions) (Figure 2).

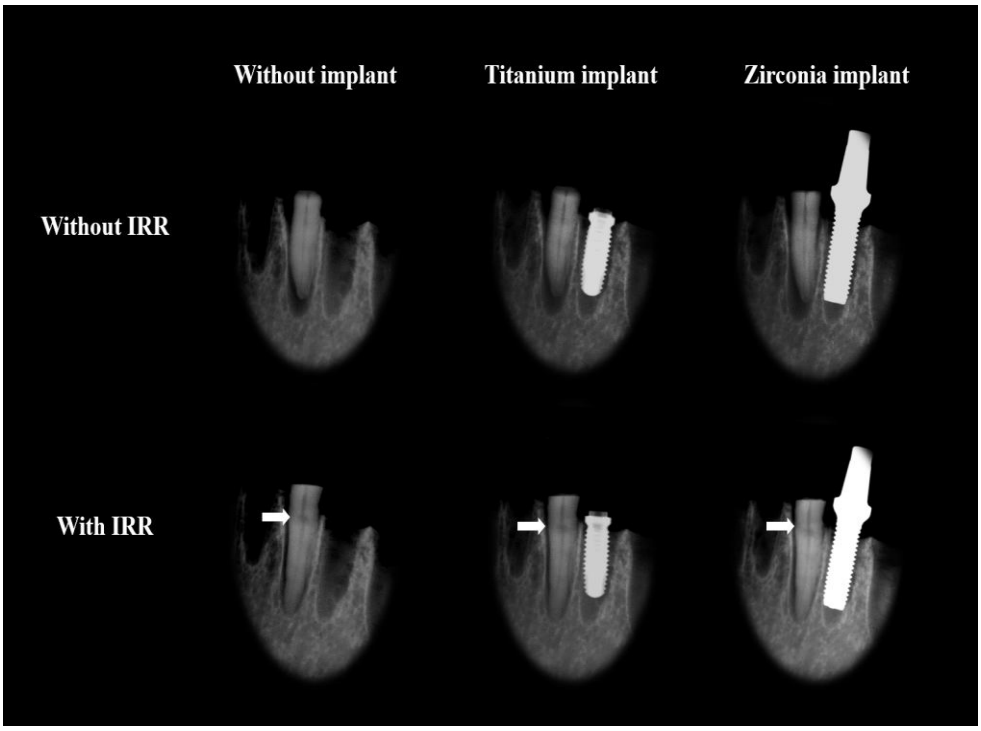


Figure 2. Periapical radiographs exhibiting teeth without and with IRR according to different conditions assessed: without implant, near a titanium implant, and near a zirconia implant

CBCT exams were obtained using the OP300 Maxio unit (Instrumentarium Dental, Tuusula, Finland). The region of interest of the mandible was centered within the field of view (FOV), and its position was standardized using the unit's guide lights. The mandible was positioned inside a plastic container filled with water to reproduce soft-tissue attenuation. Exams were acquired using a 5 × 5 cm FOV, a 0.085 mm^3 voxel size, at 90 kVp and 8 mA. Similar to the radiographic protocol, each root was scanned under three conditions, with and without the titanium and zirconia implants, resulting in 60 CBCT exams (20 roots × 3 conditions) (Figure 3).

Image evaluation

Four oral radiologists were trained in advance using periapical radiographs and CBCT exams that were not included in the study sample. After training, each examiner independently evaluated the images, first assessing the periapical radiographs and then, after a 30-day interval, the CBCT exams. This interval between the different imaging modalities was established to minimize potential recall bias from the previous evaluation. All assessments were conducted in a quiet room with low ambient lighting. Throughout the imaging assessment, the examiners were blinded to the actual number of roots presenting IRR. Sixty periapical radiographs, randomized and coded, were sent to the examiners in TIFF format. Examiners performed radiographic interpretation using JPEG View software (version 1.0.37, public domain). Each examiner analyzed up to 20 radiographs per day, with at least 24 hours between sessions. Adjustments on brightness, contrast, and the use of zoom were allowed. IRR detection was scored on a 5-point scale: 1 = definitely absent, 2 = probably absent, 3 = uncertain, 4 = probably present, and 5 = definitely present.

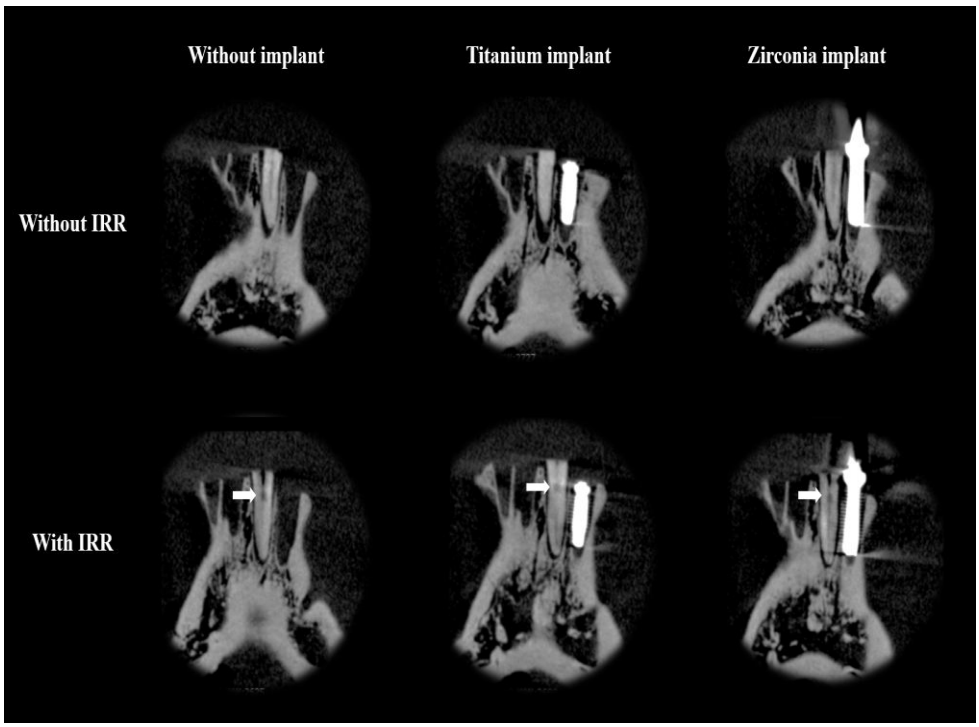


Figure 3. Coronal reconstructions of CBCT exams exhibiting teeth without and with IRR according to different conditions assessed: without implant, near a titanium implant, and near a zirconia implant

Then, the 60 CBCT exams were exported in DICOM format, randomized, and coded before being assessed by the same four examiners. Up to 20 exams were evaluated per day with a minimum 24-hour interval between sessions, using OnDemand 3D software (Cybermed, Irvine, CA, USA). As with the radiographs, post-processing adjustments were allowed, and the same 5-point scale was applied for IRR classification. Twenty days after completing these assessments, 30% of the sample was reexamined to determine intra-examiner agreement.

Statistical analysis

Statistical analyses were performed using SPSS version 25.0 (IBM Corp., Armonk, NY, USA), with a significance level of 5% ($p<0.05$). To calculate the diagnostic metrics, examiners' assessments were dichotomized into "IRR absent" (scores 1, 2, and 3) and "IRR present" (scores 4 and 5). The area under the receiver operating characteristic curve (AUC), sensitivity, and specificity values were calculated by comparing each examiner's assessment with the actual condition of each root (presence or absence of IRR). These values were then compared using two-way analysis of variance (ANOVA) with the Tukey post hoc test to assess the influences of imaging method (periapical radiograph or CBCT exams) and implant status (none, titanium or zirconia implant). Inter- and intraexaminer agreement was assessed using the weighted Kappa test and interpreted according to the Landis and Koch scale (19). Power analysis revealed that the sample size of the present study ensured statistical power of 85%. The null hypothesis stated that neither the imaging method nor the presence of implants would influence the diagnostic performance for detecting IRR, as assessed by the AUC, sensitivity, and specificity.

Results

Table 1 presents the diagnostic values (AUC, sensitivity, and specificity) for IRR according to the imaging modalities and the presence or absence of implants. Implant status did not influence the values, regardless of imaging modality ($p>0.05$). In contrast, imaging modality did influence performance. CBCT outperformed periapical radiographs in every simulated condition, demonstrating higher AUC, sensitivity, and specificity ($p=0.007$ for AUC; $p=0.009$ for sensitivity, and $p=0.037$ for specificity).

Table 1. Mean (SD) values of AUC, sensitivity, and specificity for diagnosing internal root resorption, presented according to implant presence and imaging modality

Diagnostic metric	Implant	Imaging modality*		*p value*	
		Radiograph	CBCT	Implant	Imaging modality
AUC	Without	0.70 (0.58–0.81)	0.98 (0.93–1.00)	0.816	**0.007**
	Titanium	0.77 (0.66–0.87)	0.94 (0.88–0.99)		
	Zirconia	0.76 (0.65–0.85)	0.93 (0.86–0.98)		
Sensitivity	Without	0.48 (0.40–0.56)	0.98 (0.90–1.00)	0.255	**0.009**
	Titanium	0.60 (0.46-0.74)	0.93 (0.70–1.00)		
	Zirconia	0.53 (0.36-0.70)	0.88 (0.73–0.96)		
Specificity	Without	0.83 (0.73-0.94)	0.93 (0.77–1.00)	0.115	**0.037**
	Titanium	0.88 (0.66-1.00)	0.93 (0.77–1.00)		
	Zirconia	0.93 (0.77-1.00)	0.99 (0.98–1.00)		

AUC, area under the receiver operating characteristic curve; SD, standard deviation
*Indicates statistically significant difference between imaging modality used for all the diagnostic metrics assessed according to two-way repeated measures ANOVA

Based on the AUC values and using a widely accepted scale for interpreting diagnostic performance, periapical radiographs demonstrated AUCs above 0.7, reflecting an acceptable level of discrimination. In contrast, CBCT exams showed AUC values exceeding 0.9, indicating outstanding discriminatory ability (20). Furthermore, because a diagnostic test is generally considered clinically acceptable when the sum of its sensitivity and specificity is at least 1.5, CBCT was the only imaging modality that demonstrated adequate diagnostic performance for detecting IRR. The 1.5 threshold was reached regardless of the presence of adjacent implants, reinforcing the reliability of CBCT for distinguishing teeth with IRR from those without the condition (21). Notably, the sensitivity of periapical radiographs did not exceed 0.60, underscoring a limited capacity to accurately detect the presence of IRR.

Additionally, intra-examiner agreement ranged from moderate to almost perfect (0.48–0.95), while inter-examiner agreement ranged from fair to almost perfect (0.30–0.85) (16).

Discussion

Previous studies have demonstrated that CBCT offers higher diagnostic accuracy for IRR detection than periapical radiographs (6,22). However, those investigations were conducted under ideal conditions, without the presence of materials capable of producing artifacts near the area of interest (6). In contrast, the present study investigated IRR detection in the presence of implants, and the authors initially hypothesized that beam-hardening artifacts would impair CBCT image quality enough to hinder IRR visualization, making periapical radiographs the more reliable modality. However, despite titanium and zirconia implants adjacent to the simulated IRR defects, CBCT still achieved superior diagnostic accuracy compared with periapical radiographs.

The assumption that periapical radiographs would outperform CBCT in such a scenario was based in part on a previous finding showing that very small peri-implant defects (approximately 0.35 mm in size) were more easily identified on radiographs than on CBCT exams acquired from different devices (15). Likewise, studies assessing recurrent caries lesions adjacent to amalgam restorations, which also generate beam-hardening artifacts due to their high atomic number, reported no diagnostic advantage of CBCT over intraoral radiographs when lesions were experimentally induced (13). A systematic review and meta-analysis by Ku et al. (2025) further reinforced this observation by concluding that neither modality consistently outperformed the other for identifying recurrent caries around restorations (23). Collectively, these findings differed

from the present results, in which CBCT demonstrated significantly higher accuracy for IRR detection than periapical radiographs.

One hypothesis for the discrepancy between the present study and previous investigations is the nature of the diagnostic task. In those studies, the region of interest was located much closer to the artifact-generating material. Caries lesions were assessed on proximal surfaces adjacent to teeth restored, whereas peri-implant defects involved bone loss surrounding the implant surface (13,23). Consequently, in these scenarios, the diagnostic region is more susceptible to artifact-related image impairment. For IRR, the lesion is located within the root canal space and is therefore not in such close proximity to, or direct spatial relationship with, adjacent implants. This greater distance from the artifact source may reduce the impact of the titanium or zirconia presence.

On the other hand, the present findings are consistent with studies investigating vertical root fracture detection in teeth containing metallic posts (e.g., nickel–chromium alloys) (24,25). These authors similarly reported superior diagnostic accuracy of CBCT over periapical radiographs despite artifact-generating materials (24,25). These findings suggest that, although beam hardening artifacts may reduce CBCT image quality by producing hypodense and hyperdense streaks, the modality still offers a diagnostic advantage. This advantage likely stems from its ability to depict anatomical structures without superimposition, together with its superior spatial resolution, which may outweigh the negative effects of artifact-related alterations. This benefit appears to persist across different diagnostic tasks, such as root fractures or IRR.

The selected exposure parameters produced images with appropriate brightness and contrast, ensuring adequate conditions for interpretation (26). A receptor holder was used not only to standardize image geometry but also to reduce the likelihood of radiographic retakes, which, in a clinical context, would unnecessarily increase the X-radiation dose to the patient. Comparable attention was given to CBCT acquisition parameters. A small FOV and an intermediate mA setting were chosen, as larger FOVs and higher mA values substantially increase radiation exposure (27).

Another potential dose-reduction strategy in CBCT imaging is activating the metal artifact reduction (MAR) algorithm. MAR operates during image reconstruction by homogenizing discrepant gray values to mitigate the appearance of artifacts (12,28). However, evidence regarding its diagnostic impact is mixed. Some authors report that MAR can enhance the diagnostic accuracy for vertical root fracture detection, whereas its influence on horizontal root fracture diagnosis, particularly when fractures are located near implants, appears limited (28,29). Interestingly, other authors observed that MAR activation reduced the negative effects caused by the presence of two metallic posts adjacent to a region suspected of IRR (10). The use of MAR was not assessed herein due to its limited availability across different CBCT devices and to the fact that the primary goal was to determine whether the presence of implants compromises the accuracy of IRR detection on CBCT examinations. Nevertheless, the authors acknowledge the need for future studies specifically investigating how MAR may influence the diagnosis of IRR in regions adjacent to dental implants. Further research should also evaluate different CBCT systems to better understand the possible influence of the selected X-ray unit.

Although CBCT demonstrated superior diagnostic accuracy to periapical radiographs for detecting IRR in the present study, this does not imply that CBCT should be used as the first-line imaging modality in clinical practice (5,30). Periapical radiographs remain the recommended initial imaging examination for suspected IRR, as some lesions, particularly those of moderate to large size, can be adequately visualized on two-dimensional imaging. CBCT should be considered only when periapical radiographs, combined with clinical findings and patient history, yield inconclusive information or when three-dimensional assessment is expected to influence treatment planning (5). CBCT provides clinically relevant details about the extent, depth, and possible perforation associated with IRR, which may be critical for decision-making (5,30). The key contribution in the present study is the demonstration that, even in the presence of titanium and zirconia implants, CBCT remains capable of providing reliable diagnostic information about IRR. This reinforces the modality's value as a second-line imaging tool when conventional radiographs do not offer sufficient diagnostic clarity.

This investigation was conducted as an *ex vivo* study, a methodological design that does not account for certain patient-related factors, such as motion artifacts occurring during image acquisition. However, only under *ex vivo* conditions would it be possible to obtain multiple periapical radiographs and CBCT exams of the same teeth while maintaining strict standardization of exposure parameters and evaluation conditions. To better approximate clinical reality, during periapical radiographic acquisition, the mandible was covered with a 15-mm layer of wax to simulate soft-tissue attenuation (31). For CBCT imaging, the mandible was immersed in a plastic container filled with water (28,29). Given that the literature reports a higher prevalence of IRR in incisor teeth, the sample consisted of single-rooted teeth positioned in the socket corresponding to the left mandibular lateral incisor. All simulated lesions were small in order to increase the difficulty of the diagnostic task (1). This design aimed to reproduce a clinically relevant scenario by reflecting the tooth most commonly affected by IRR while also creating a more challenging condition for image interpretation. In addition, although inter-examiner agreement was relatively low compared with intra-examiner agreement, both values were higher than those reported in previous studies, supporting the reliability of the present results (17,32).

Since an intermediate mA setting (8 mA) was used herein, future work could explore the diagnostic performance of CBCT at lower mA values to better understand how exposure parameters influence IRR detection. Should reduced mA settings continue to yield high diagnostic accuracy, this would support lowering the radiation dose to the patient without compromising diagnostic accuracy (16). Finally, longitudinal studies comparing treatment success, tooth retention, and patient-reported outcomes in IRR cases diagnosed using CBCT versus periapical radiographs would also provide robust evidence to guide clinical decision-making. Although such studies pose methodological challenges, these studies combined with the present research could contribute to the development of evidence-based diagnostic guidelines.

Conclusion

CBCT demonstrated higher diagnostic accuracy than periapical radiography for detecting IRR, and the presence of dental implants did not significantly affect its performance. When periapical radiography is inconclusive in suspected cases of IRR, CBCT may serve as a valuable adjunctive imaging method, even in regions adjacent to implants. However, CBCT should be considered a second-line modality and used only when clinically justified, in accordance with radiation protection principles.

Conflict of Interest
The authors declare that they have no conflict of interest.

Data Availability
The research data are available upon request.

Responsible Editor
Manoel Damião Sousa-Neto

Resumo

O estudo comparou a acurácia de diagnóstico da tomografia computadorizada de feixe cônico (TCFC) e da radiografia periapical na detecção de reabsorção radicular interna (RRI) em dentes adjacentes a implantes de titânio ou zircônia. Vinte dentes unirradiculares (10 com RRI e 10 sem) foram posicionados individualmente em uma mandíbula humana. Radiografias periapicais e exames de TCFC foram obtidos com e sem implantes. As radiografias foram adquiridas utilizando uma placa de fósforo fotoestimulável, com parâmetros de 70 kVp, 7 mA e 0,160 s. Os exames de TCFC foram realizados com 90 kVp, 8 mA, tamanho de voxel de 0,085 mm³ e campo de visão de 5×5 cm. Quatro examinadores avaliaram independentemente todas as imagens. A área sob a curva ROC (AUC), sensibilidade e especificidade foram calculados e comparados por meio de ANOVA dois

fatores (α=5%). A concordância intra e interexaminadores para o diagnóstico de RRI foi avaliada utilizando o coeficiente Kappa ponderado. A TCFC apresentou valores significativamente mais elevados de AUC (p=0,007), sensibilidade(p=0,009) e especificidade (p=0,037) para a detecção de RRI em comparação com a radiografia periapical, independentemente da presença ou do tipo de implante. A presença do implante não influenciou os resultados tanto para a TCFC quanto para a radiografia periapical. A concordância intraexaminador variou de moderada a quase perfeita (0,48–0,95), e a concordância interexaminador variou de razoável a quase perfeita (0,30–0,85). A TCFC demonstrou maior acurácia do que a radiografia periapical para a detecção de RRI, mesmo na presença de implantes de titânio ou zircônia, uma vez que os artefatos associados aos implantes não prejudicaram a interpretação dos exames. Portanto, quando a radiografia periapical for insuficiente para se estabelecer um diagnóstico, a TCFC pode ser clinicamente justificada apesar da exposição adicional à radiação.

References

1. Patel S, Ricucci D, Durak C, Tay F. Internal root resorption: a review. J Endod. 2010;36:1107-21.
2. Fuss Z, Tsesis I, Lin S. Root resorption--diagnosis, classification and treatment choices based on stimulation factors. Dent Traumatol. 2003;19:175-82.
3. Patel S, Saberi N, Pimental T, Teng PH. Present status and future directions: Root resorption. Int Endod J. 2022;55:892-921.
4. Madani Z, Moudi E, Bijani A, Mahmoudi E. Diagnostic Accuracy of Cone-Beam Computed Tomography and Periapical Radiography in Internal Root Resorption. Iran Endod J. 2016;11:51-6.
5. Sousa Melo SL, Fayad MI, Gohel A, Johnson BR, Kalathingal S, Mahdian M, Nair M, Setzer FC, Makins SR. AAE and AAOMR Joint Position Statement: Use of Cone-Beam Computed Tomography in Endodontics 2025 Update. J Endod. 2026;52:4-13.
6. Patel S, Dawood A, Wilson R, Horner K, Mannocci F. The detection and management of root resorption lesions using intraoral radiography and cone beam computed tomography - an in vivo investigation. Int Endod J. 2009;42:831-38.
7. Creanga AG, Geha H, Sankar V, Teixeira FB, McMahan CA, Noujeim M. Accuracy of digital periapical radiography and cone-beam computed tomography in detecting external root resorption. Imaging Sci Dent. 2015;45:153-8.
8. Durack C, Patel S, Davies J, Wilson R, Mannocci F. Diagnostic accuracy of small volume cone beam computed tomography and intraoral periapical radiography for the detection of simulated external inflammatory root resorption. Int Endod J. 2011;44:136-47.
9. Schulze R, Heil U, Gross D, et al. Artefacts in CBCT: a review. Dentomaxillofac Radiol. 2011;40:265-73.
10. Gaêta-Araujo H, Nascimento EHL, Oliveira-Santos N, Pinheiro MCR, Coelho-Silva F, Oliveira-Santos C. Influence of adjacent teeth restored with metal posts in the detection of simulated internal root resorption using CBCT. Int Endod J. 2020;53:1299-306.
11. Freitas DQ, Vasconcelos TV, Noujeim M. Diagnosis of vertical root fracture in teeth close and distant to implant: an in vitro study to assess the influence of artifacts produced in cone beam computed tomography. Clin Oral Investig. 2019;23:1263-70.
12. Gonzalez-Passos T, Barros-Costa M, Oliveira ML, Freitas DQ. Influence of tube current and metal artifact reduction on the diagnosis of external cervical resorption in teeth adjacent to a dental implant in CBCT: an ex-vivo study. Clin Oral Investig. 2024;28:356.
13. Sousa Melo SL, Belem MDF, Prieto LT, Tabchoury CPM, Haiter-Neto F. Comparison of cone beam computed tomography and digital intraoral radiography performance in the detection of artificially induced recurrent caries-like lesions. Oral Surg Oral Med Oral Pathol Oral Radiol. 2017;124:306-14.
14. Ruiz DC, Reis LO, Fontenele RC, Miranda-Viana M, Farias-Gomes A, Freitas DQ. Influence of an adjacent zirconium implant, tube current, and metal artifact reduction algorithm on horizontal root fracture diagnosis in cone beam computed tomography. Oral Surg Oral Med Oral Pathol Oral Radiol. 2024;137:190-8.

15. Dave M, Davies J, Wilson R, Palmer R. A comparison of cone beam computed tomography and conventional periapical radiography at detecting peri-implant bone defects. Clin Oral Implants Res. 2013;24:671-8.
16. Oenning AC, Jacobs R, Salmon B, & DIMITRA Research Group (http://www.dimitra.be) (2021). ALADAIP, beyond ALARA and towards personalized optimization for paediatric cone-beam CT. International Journal of Paediatric Dentistry, 31, 676–78.
17. Oliveira-Santos N, Gaêta-Araujo H, Ruiz DC, Nascimento EHL, Cral WG, Oliveira-Santos C, Groppo FC. The impact of digital filters on the diagnosis of simulated root resorptions in digital radiographic systems. Clin Oral Investig. 2022;26:4743-52.
18. Nascimento EHL, Gaêta-Araujo H, Galvão NS, Moreira-Souza L, Oliveira-Santos C, Freitas DQ. Effect of brightness and contrast variation for detectability of root resorption lesions in digital intraoral radiographs. Clin Oral Investig. 2019;23:3379-86.
19. Landis JR, Koch GG. The measurement of observer agreement for categorical data. Biometrics. 1977;33:159-74.
20. Hosmer DW Jr, Lemeshow S, Sturdivant RX. Applied Logistic Regression. 3rd ed. New York, NY: Wiley; 2013:177.
21. Power M, Fell G, Wright M. Principles for high-quality, highvalue testing. Evid Based Med. 2013; 18:5-10.
22. Lima TF, Gamba TO, Zaia AA, Soares AJ. Evaluation of cone beam computed tomography and periapical radiography in the diagnosis of root resorption. Aust Dent J. 2016;61:425-31.
23. Ku JC, Lam WY, Li KY, Hsung RT, Chu CH, Yu OY. Accuracy of detection methods for secondary caries around direct restorations: A systematic review and meta-analysis. J Dent. 2025;153:105541.
24. Junqueira RB, Verner FS, Campos CN, Devito KL, do Carmo AM. Detection of vertical root fractures in the presence of intracanal metallic post: a comparison between periapical radiography and cone-beam computed tomography. J Endod. 2013;39:1620-4.
25. Takeshita WM, Iwaki LC, da Silva MC, Sabio S, Albino PR. Comparison of periapical radiography with cone beam computed tomography in the diagnosis of vertical root fractures in teeth with metallic post. J Conserv Dent. 2014;17:225-9.
26. Ruiz DC, Haiter-Neto F, Gaêta-Araujo H, Freitas DQ. Does the disinfection of a photostimulable phosphor plate receptor with peracetic acid impair carious lesions diagnosis? Dentomaxillofac Radiol. 2025;24:twaf067.
27. da Silva Moura W, Chiqueto K, Pithon GM, Neves LS, Castro R, Henriques JFC. Factors influencing the effective dose associated with CBCT: a systematic review. Clin Oral Investig. 2019;23:1319-30.
28. Ruiz DC, Rosado LPL, Fontenele RC, Farias-Gomes A, Freitas DQ. Vertical root fracture diagnosis in teeth with metallic posts: Impact of metal artifact reduction and sharpening filters. Imaging Sci Dent. 2024;54:139-45.
29. Ruiz DC, de Oliveira Reis L, Fontenele RC, Miranda-Viana M, Farias-Gomes A, Freitas DQ. Combination of metal artifact reduction and sharpening filter application for horizontal root fracture diagnosis in teeth adjacent to a zirconia implant. Imaging Sci Dent. 2024;54:289-95.
30. Patel S, Krastl G, Weiger R, Lambrechts P, Tjäderhane L, Gambarini G, Teng PH. ESE position statement on root resorption. Int Endod J. 2023;56:792-801.
31. Soltani P, Devlin H, Aydin U, Tafti KT, Baghaei K. Soft tissue simulant materials in X-ray-based imaging in dentomaxillofacial radiology: a scoping review. Oral Radiol. 2024;40:109-23.
32. Miranda-Viana M, Madlum DV, Oliveira-Santos N, Gaêta-Araujo H, Haiter-Neto F, Oliveira ML. Influence of the image file format of digital periapical radiographs on the diagnosis of external and internal root resorptions. Clin Oral Investig. 2021;25:4941-48.

Received: 12/02/2026
Accepted: 08/07/2026